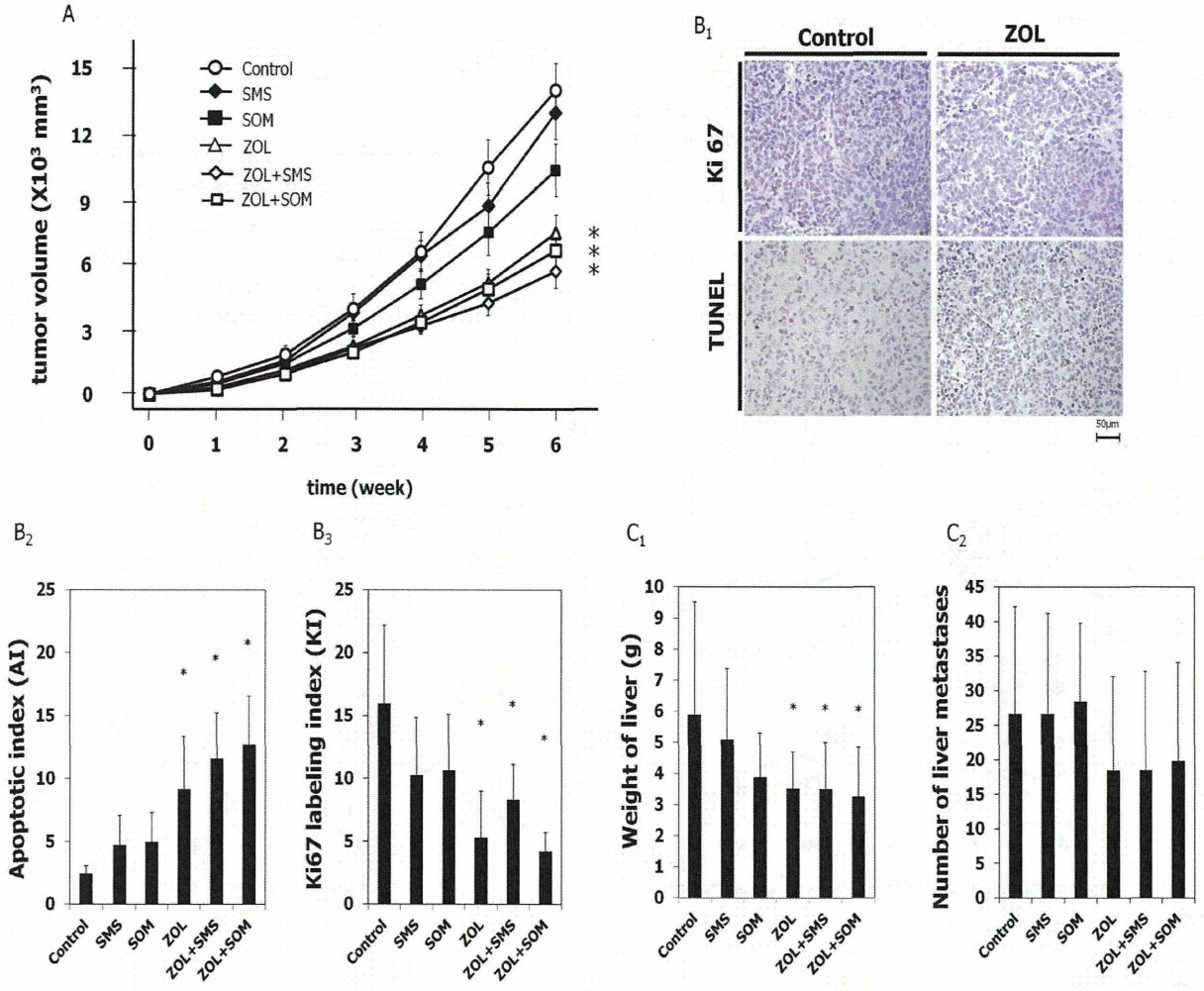

Fig. 2. Effects of ZOL, SMS, and SOM as single agents and in combination on subcutaneous inoculated NE-10 allografts. Six-week-old male BALB/c nude mice were castrated. After one week, 50 mg tissue fragments from the NE-10 allograft model were subcutaneously inoculated into the backs of mice. For 2 weeks, NE-10 tumors were allowed to grow to approximately more than 100 mm^3 before randomization into six treatment groups: control, ZOL, SMS, SOM, ZOL plus SMS, and ZOL plus SOM (n = 13/group). NE-10 allografts in each group were treated for 6 weeks. **A**: Growth of NE-10 tumors in mice treated with ZOL, ZOL plus SMS, and ZOL plus SOM was significantly slowed compared to the saline control ($P = 0.003$, $P < 0.001$, and $P = 0.001$, respectively). Data are means; bars ± SE; *, significantly different from control group ($P < 0.05$; repeated-measures ANOVA). **B**: Effects of ZOL, SMS and SOM as single agents and in combination on apoptosis and cell cycle progression. Immunohistochemical staining was done by usingTUNEL and Ki67 staining (**B_1**). Apoptoic effects were measured by the number of TUNEL-positive cells per 1,000 cells, apoptoic index (AI). The AI was significantly increased in tumors from mice treated with ZOL, ZOL plus SMS, or ZOL plus SOM compared to the control (means: 9.2, 11.6, and 12.7, respectively, vs. 2.4) (**B_2**). Cell cycle progression was measured by the number of Ki67-positive cells per 1,000 cells (KI: Ki-67 labeling index). The KI was significantly decreased in tumors from mice treated with ZOL, ZOL plus SMS, or ZOL plus SOM compared to the control (means: 5.3, 8.3, and 4.2, respectively, vs. 15.9) (**B_3**). Data are means; bars ± SD; *, significantly different from control group ($P < 0.05$; one-way ANOVA). **C**: Effects of ZOL, SMS and SOM as single agents and in combination on liver metastases. The weights of livers having metastatic nodules in ZOL, ZOL plus SMS, or ZOL plus SOM were significantly lower than for the control (**C_1**). The numbers of metastatic nodules in these groups were not significantly different from the control (**C_2**). Data are means; bars ± SD. *, Significantly different from control group ($P < 0.05$; one-way ANOVA).

weights of livers having metastatic nodules in ZOL, ZOL plus SMS, or ZOL plus SOM were significantly lower than for the control (Fig. $2C_1$), but the numbers of metastatic nodules in these groups were not significantly different from the control (Fig. $2C_2$).

Effects of ZOL, SMS and SOM as Single Agents and in Combination on Growth of NE-CS Cells In Vitro

We investigated the inhibitory effects of ZOL, SMS, and SOM, alone and in combination on proliferation

of NE-CS cells. Cell viability was measured by the WST-8 assay when NE-CS cells were treated with various concentrations of ZOL, SMS and SOM (0.1–100 μmol/L) in the treatment groups for 24, 48 or 72 hr. For combinations, the same concentrations of ZOL and SMS or SOM were used. The IC50 for ZOL at 72 hr was 15.7 μmol/L, whereas those for ZOL plus SMS, and ZOL plus SOM were 14.1, and 13.5 μmol/L, respectively (Fig. 3A). The combination of ZOL and somatostatin analogs did not demonstrate synergistic effects (CI: 0.57–1.00). ZOL induced time- and dose-dependent proliferative inhibition of NE-CS cells (Fig. 3B). These effects of ZOL were reversed by 20 μmol/L of FOH (Fig. 3C).

ZOL Inhibits Cell Cycle Activity and Induces Apoptosis of NE-CS Cells

TUNEL-positive cells, indicated in red, increased with increased concentrations of ZOL. On the other hand, Ki-67-positive cells, colored green, decreased (Fig. 4A). We also analyzed the AI and KI with ZOL

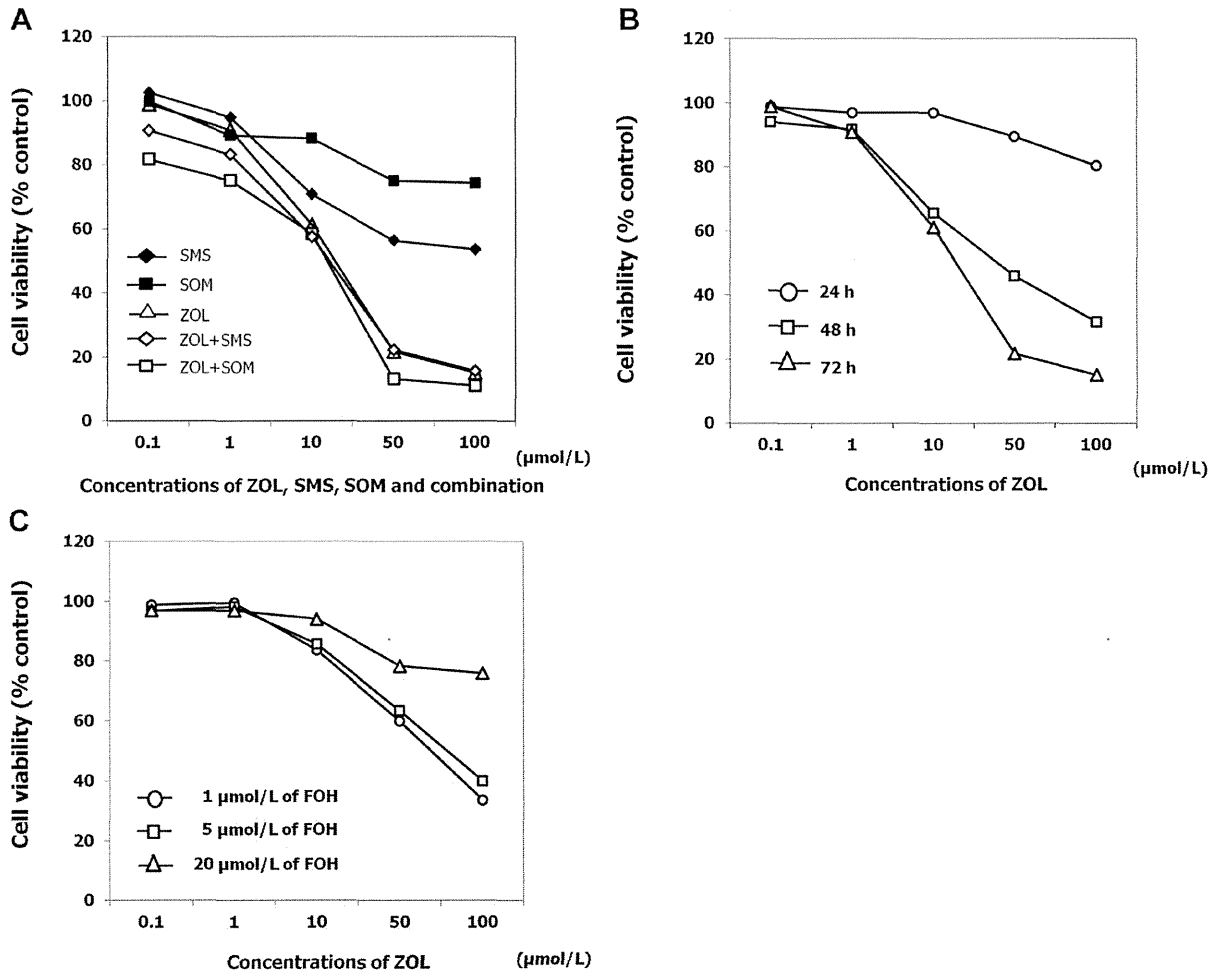

Fig. 3. Effects of ZOL, SMS and SOM as single agents and in combination on growth of NE-CS cells. Cell viability was measured by WST-8 assay when NE-CS cells were treated with various concentrations of ZOL, SMS and SOM (0.1–100 μmol/L) for 24, 48 or 72 hr. For combination, the same concentrations of ZOL and SMS or SOM were used. Cell viability was also measured when NE-CS cells were treated for 48 hr with the indicated concentrations (from 0.1 to 100 μmol/L) of ZOL plus 1, 5, and 20 μmol/L of farnesyl-pyrophosphate ammonium salt (FOH) (n = 5/group). **A**: Cell viability of NE-CS cells at 72 hr in each treatment group. The IC50 of ZOL at 72 hr for NE-CS cells was 15.7 μmol/L for ZOL, whereas it was 14.1 μmol/L for ZOL plus SMS, and 13.5 μmol/L for ZOL plus SOM. The combination of ZOL and somatostatin analogs did not create synergistic effects. **B**: Cell viability of NE-CS cells in time- and dose-dependent manners. ZOL induced time- and dose-dependent proliferative inhibition of NE-CS cells. **C**: Cell viability of NE-CS cells at 48 hr in ZOL plus FOH. ZOL-induced inhibition was reversed by 20 μmol/L of FOH.

concentrations of 0, 10, 50, and 100 μmol/L. The AI was significantly increased in ZOL 50, and 100 μmol/L compared to the control (means: 55.7 and 136.5, respectively, vs. 13.8) (Fig. 4B). The KI was significantly decreased in ZOL 10, 50, and 100 μmol/L compared to the control (means: 37.6, 22.8, and 1.3, respectively, vs. 68.7) (Fig. 4C).

ZOL Inhibits Migration of NE-CS Cells

In addition to effects of ZOL on cell cycle activity and apoptosis, we examined whether ZOL inhibited migration of NE-CS cells, using a Boyden chamber assay. NE-CS cells, with or without ZOL concentrations of 10, and 100 μmol/L, that migrated across the pores at 2, 4, 6 and 8 hr were counted. The numbers of cells migrating 1 mm^{-2} of membrane were significantly decreased in ZOL 10, and 100 μmol/L (Fig. 5A). When culture medium adding 20 μmol/L of FOH was incubated in upper chamber, the ZOL-induced inhibition was not appeared (Fig. 5B).

ZOL Utilizes the Ras/MAPK Pathway via the Mevalonate Pathway in NE-CS Cells

Since ZOL inhibits farnesyl-pyrophosphate synthetase in the mevalonate pathway and impairs prenylation of Ras, we evaluated the effects of ZOL on Ras activity. We used FOH, which potentially induces farnesylation of Ras. As evaluated by pull-down assay, 10, and 100 μmol/L inhibited Ras activation in NE-CS cells, and then the ZOL-induced inhibition was reversed by FOH (Fig. 6). We examined the effects of ZOL on Erk-1/2, which are the terminal proteins of the Ras/MAPK pathway. ZOL inhibited Erk1/2 phosphorylation as evaluated by Western blot assay.

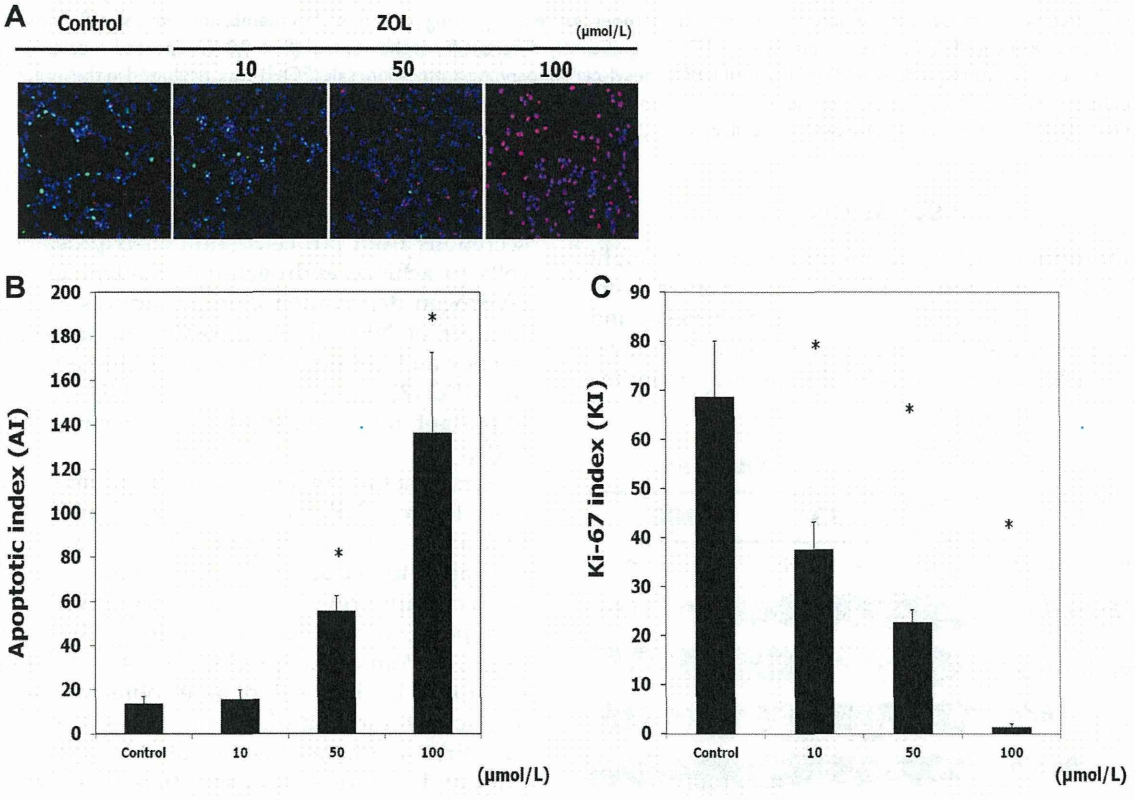

Fig. 4. Effects of ZOL on apoptosis and cell activity of NE-CS cells. **A**: TUNEL and anti-Ki67 immunofluorescence were used for NE-CS cells treated with ZOL concentrations of 0, 10, 50, and 100 μmol/L (n = 5/group). DAPI was used to visualize cell nuclei. TUNEL-positive cells, colored red, increased with increased concentrations of ZOL. On the other hand, Ki-67-positive cells, colored green, decreased. **B**: The numbers of TUNEL-positive cells per 1,000 cells apoptoic index (AI) were significantly increased in ZOL 50, and 100 μmol/L compared to the control (means: 55.7, and 136.5, respectively, vs. 13.8). Data are means; bars ± SD; *, significantly different from control group ($P < 0.001$; Student's *t*-test). **C**: The numbers of Ki67-positive cells per 1,000 cells (KI: Ki-67 labeling index) were significantly decreased in ZOL 10, 50, and 100 μmol/L compared to the control (means: 37.6, 22.8, and 1.3, respectively, vs. 68.7). Data are means; bars ± SD; *, significantly different from control group ($P < 0.001$; Student's *t*-test).

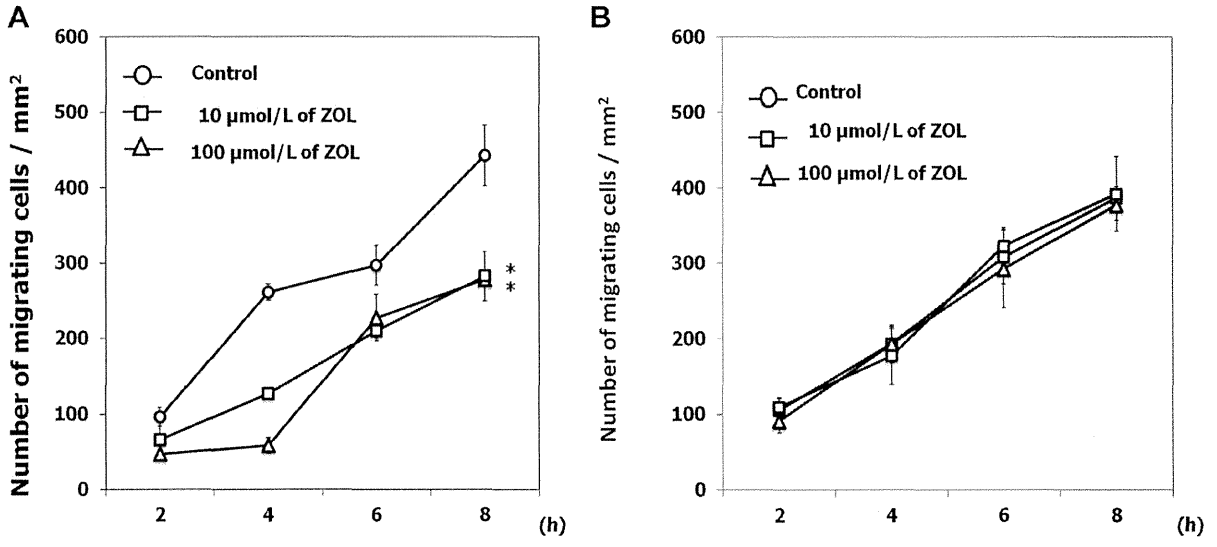

Fig. 5. Effects of ZOL on migration of NE-CS cells. Migration assay was performed by using a Boyden chamber (n = 3/group). **A**: In experiment I, NE-CS cells (1×10^5) were placed in the upper chamber with 100 μl of culture medium with or without ZOL (10, 100 μmol/L). In the lower chamber, 600 μl of culture medium was added. The numbers of cells migrating per 1 mm^{-2} of membrane were significantly decreased in ZOL 10, and 100 μmol/L. Data are means; bars ± SD; *, significantly different from the control ($P < 0.001$; repeated-measures ANOVA). B: In experiment 2, culture medium adding 20 μmol/L of farnesyl-pyrophosphate ammonium salt (FOH) was incubated in the upper chamber. The numbers of cells migrating 1 mm^{-2} of membrane were not significantly decreased in ZOL 10, and 100 μmol/L. Data are means; bars ± SD. *, Significantly different from the control ($P < 0.001$; repeated-measures ANOVA).

DISCUSSION

Inappropriate NE regulation in the prostate might facilitate carcinogenesis, proliferation and other tissue changes such as loss of basal cells, angiogenesis, and piling up of prostatic luminal epithelium and invasion, which are characteristic of prostatic carcinoma [20]. In addition, we previously demonstrated that secretions from NE cells stimulated prostatic cancer cells to achieve androgen-independent growth [21]. Androgen deprivation therapy induces an increased number of NE cells in prostate cancer and the frequency and density of NE cells are more pronounced in CRPC [22]. Thus, the control of NE cells might be important for establishing a treatment strategy for CRPC.

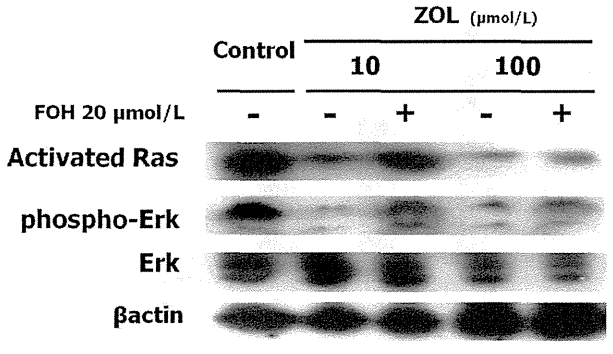

Fig. 6. Effects of ZOL on Ras/MAPK pathway of NE-CS cells. We used farnesyl-pyrophosphate ammonium salt (FOH), which potentially induces farnesylation of Ras. Ras activity was evaluated by pull-down assay, and Erk activity by Western blot assay. As evaluated by pull-down assay, 10, and 100 μmol/L ZOL inhibited Ras activation in NE-CS cells, and then the ZOL-induced inhibition was reversed by FOH. ZOL inhibited Erk1/2 phosphorylation in NE-CS cells as evaluated by Western blot assay.

Somatostatin analogs have been used clinically used to treat NE tumors [23]. SMS and lanreotide, which have high affinity to SSTR2a, have been demonstrated to reduce excessive hormone production and accompanying symptoms from carcinoid tumors and pancreatic endocrine tumors such as glucagonoma, VIPoma and gastrinoma [14]. The anticancer effect may be the result of antiproliferative and apoptoic actions through direct and indirect mechanisms. The direct mechanism is mediated by SSTR on tumor cells, and suppression of secretion of several growth factors such as insulin-like growth factor-1 (IGF-1) may also indirectly inhibit the tumor growth [24–26]. In this study, in spite of the expression of SSTR2a and SSTR5 in our NE carcinoma models, we failed to find significant antiproliferative effects of SMS or SOM monotherapy in vitro or in vivo. In addition, the combination therapy with ZOL did not create a synergistic effect. Although, the exact reason is unclear, both

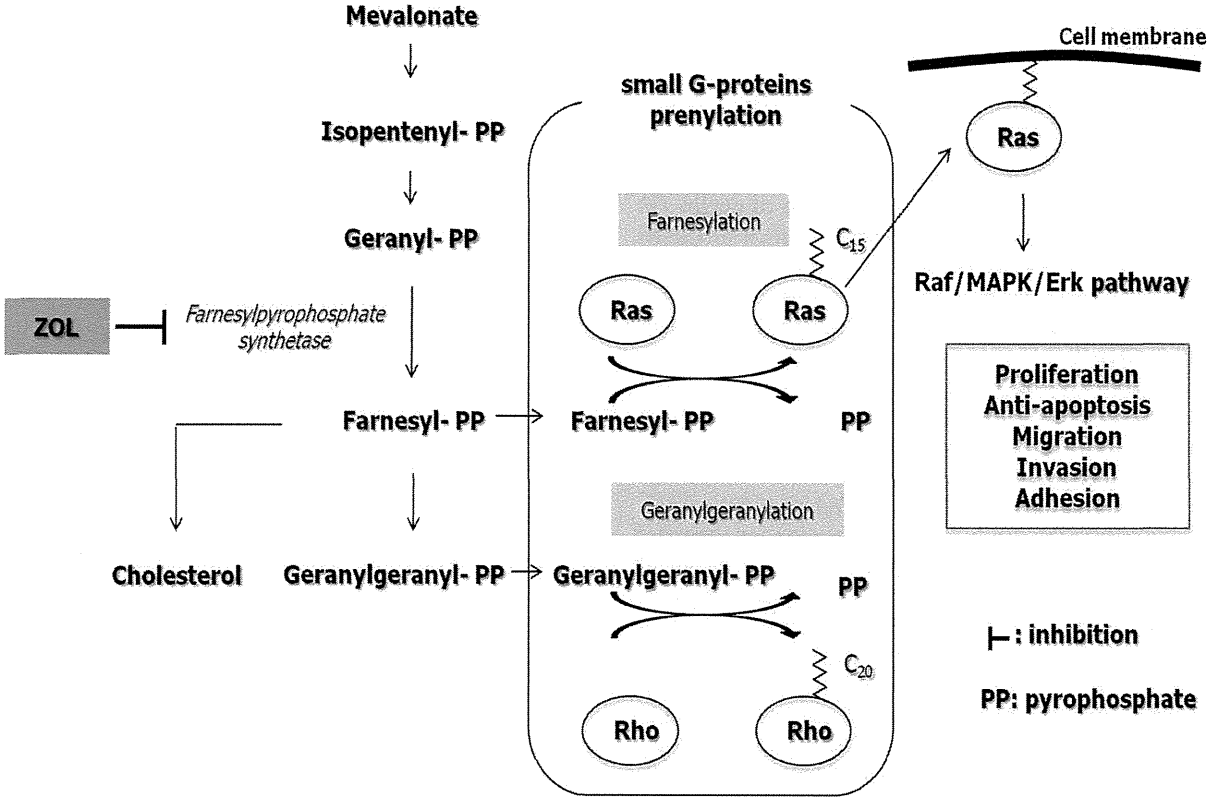

Fig. 7. Schematic representation of the mevalonate pathway and proposed mechanism of anti-tumor effects of zoledronic acid in prostatic NE carcinoma.

SMS and SOM might be insufficient to control our NE carcinoma models through autocrine, paracrine and endocrine regulation via SSTRs.

Our results suggest that ZOL induces time- and dose-dependent antiproliferative and apoptoic effects in prostatic NE carcinoma. The observed anticancer activity was exerted at ZOL IC50 levels of from 15.8 to 36.0 μmol/L. In addition, the drug reduced migration by 8 hr in vitro even at the 10 μmol/L concentration, and the time and dose did not seem to affect the viability of cells. These effects were caused by disruption of prenylation of Ras proteins as a result of farnesyl-pyrophosphate synthetase inhibition, disrupting the downstream MAPK/Erk signaling pathway (Fig. 7). Farnesyl-pyrophosphate synthetase is a key enzyme in the mevalonate pathway, which produces essential lipid molecules such as cholesterol, farnesyl-pyrophosphate and geranylgeranyl-pyrophosphate [27]. Small G proteins need prenylation to link to the inner surface of the cell membrane and function in signal translation [28]. Prenylation of small G proteins involves farnesylation, which provides a 15-carbon isoprenoid moiety with Ras, and geranylgeranylation, which provides a 20-carbon isoprenoid moiety with Rap Rac or Rho [27,28]. Ras is the most thoroughly characterized member of the small G proteins involved in key oncogenic cellular processes such as proliferation, anti-apoptosis, migration, invasion and adhesion (Fig. 7). Therefore, it is anticipated that ZOL disturbing prenylation of Ras will induce multifactorial anticancer effects in cancer cells.

Several studies had shown that ZOL induces apoptosis via impaired prenylation of small G proteins in various cancer cells, including prostate [12,29–31], breast [32,33], myeloma [34], colon [35], and lung cancer cell lines [36]. Caraglia et al. [12] reported the effects of the combination of ZOL and farnesyl-transferase inhibitor R115777 on PC3 and DU145 prostate cancer cell lines. These effects paralleled disruption of Ras/MAPK/Erk and Akt survival pathways, which consequently decreased phosphorylation of both mitochondrial bcl-2 and bad proteins, and caspase activation. These findings may support our results indicating that ZOL induced apoptosis of NE cells. Recents studies have shown that impaired geranylgeranylation on other small G proteins such as Rap1 [29,34] and RhoA [32] is also crucial for the association with these apoptotic actions induced by ZOL.

We also demonstrated that ZOL induced cell cycle arrest of the NE carcinoma cells. Both in vitro, and in

vivo, ZOL reduced the numbers of Ki67-positive cells during all active phases of the cell cycle (G1, S, G2, and M). ZOL has been shown to reduce the expression of cyclin D1 and cyclin E in osteosarcoma cells, resulting in a cell cycle block at G1, and S [37]. In addition, experiments using leukemia cells have shown that ZOL can also reduce the expression of cyclin D3 and cyclin B, resulting in a cell cycle block at G2-M [38]. These actions are suggested to occur in a p53-independent manner followed by subsequent apoptosis. Our results indicated that ZOL inhibited the cell cycle of NE cells.

Moreover, we demonstrated that ZOL inhibited migration of NE-CS cells. It decreased the weights of livers having metastatic nodules in castrated NE-10 allografts, which means to suppress liver metastases. Likewise, Hiraga et al. [39] reported that 1 μmol/L ZOL significantly inhibited cell invasion in a breast cancer cell line (4T1/Luc), which consequently led to suppression of liver and bone metastases. Similar results were also observed in prostate cancer cell lines LNCaP, PC3, and DU145 31. In addition, Coxon et al. [40] reported an inhibitory effect of 1 μmol/L ZOL on adhesion to mineralized matrix in PC3, and DU145 cells. Although the exact mechanisms underlying these effects remain unclear, it is suggested that ZOL could inhibit several matrix metalloproteinase or adhesion molecules via impairment of prenylation of small G proteins. It is noteworthy that ZOL also inhibits essential steps for the spread of cancer cells. In addition, recent reports have shown that ZOL indirectly exerts anticancer effects via elevated function of gamma delta T cells [41,42]. It is suggested that accumulation of isopentenyl-pyrophosphate caused by ZOL may be involved in activation of gamma delta T cells [43].

There are some limitations in this study. The NE-10 allograft and the NE-CS cell line were derived from the mouse prostate. The role of human NE cells in human prostate cancer may be different from that of mouse NE cells. In addition, the characteristics of the established cell line, NE-CS, could be different from those of the original NE-10 allograft because cells suitable for survival in vitro were selected during establishment of the cell line. However, there are no ideal human lines for which both in vitro, and in vivo NE carcinoma models are available. In addition, the concentration of ZOL that induced anticancer effects in our experiments was high in comparison to the peak plasma levels (393 ± 100 ng/ml) usually achieved by intravenous infusion in patients [44]. Anticancer effects of ZOL might be considered to be exerted basically in bone metastatic lesions in which high concentrations of ZOL are achieved.

In patients with bone metastasis of prostate cancer, ZOL is commonly used for relieving pain and preventing skeletal-related events. This study revealed effects of ZOL on NE cells, potential triggers of prostate cancer leading to CRPC. Regulating the microenvironment between NE cells and prostate cancer cells may result in benefits to patients who do not have clinically detected bone metastasis. We believe that our results support the clinical rationale for earlier proactive use of ZOL, though further studies will be needed to confirm this.

CONCLUSION

We examined the in vitro, and in vivo anti-tumor effects of ZOL and somatostatin analogs (SMS and SOM) on NE carcinoma models. Our results indicate that ZOL, but not SMS or SOM, induces apoptosis and inhibition of proliferation and migration through impaired prenylation of Ras. Our findings support the possibility that ZOL could be used in the early phase for controlling NE cells which may trigger progression of prostate cancer to CRPC.

REFERENCES

1. Jemal A, Bray F, Center MM, Ferlay J, Ward E, Forman D. Global cancer statistics. CA Cancer J Clin 2011;61(2):69–90.
2. Heidenreich A, Aus G, Bolla M, Joniau S, Matveev VB, Schmid HP, Zattoni F. EAU guidelines on prostate cancer. Eur Urol 2008;53(1):68–80.
3. Debes JD, Tindall DJ. Mechanisms of androgen-refractory prostate cancer. N Engl J Med 2004;351(15):1488–1490.
4. di Sant'Agnese PA. Neuroendocrine differentiation in prostatic carcinoma: An update. Prostate Suppl 1998;8:74–79.
5. Ito T, Yamamoto S, Ohno Y, Namiki K, Aizawa T, Akiyama A, Tachibana M. Up-regulation of neuroendocrine differentiation in prostate cancer after androgen deprivation therapy, degree and androgen independence. Oncol Rep 2001;8(6):1221–1224.
6. Hirano D, Okada Y, Minei S, Takimoto Y, Nemoto N. Neuroendocrine differentiation in hormone refractory prostate cancer following androgen deprivation therapy. Eur Urol 2004;45(5):586–592; discussion 592.
7. Masumori N, Thomas TZ, Chaurand P, Case T, Paul M, Kasper S, Tsukamoto T, Shappell SB, Matusik RJ. A probasin–Large T antigen transgenic mouse line develops prostate adenocarcinoma and neuroendocrine carcinoma with metastatic potential. Cancer Res 2001;61(5):2239–2249.
8. Masumori N, Tsuchiya K, Tu WH, Lee C, Kasper S, Tsukamoto T, Shappell SB, Matusik RJ. An allograft model of androgen independent prostatic neuroendocrine carcinoma derived from a large probasin promoter-T antigen transgenic mouse line. J Urol 2004;171(1):439–442.
9. Uchida K, Masumori N, Takahashi A, Itoh N, Tsukamoto T. Characterization of prostatic neuroendocrine cell line established from neuroendocrine carcinoma of transgenic mouse allograft model. Prostate 2005;62(1):40–48.

10. Uchida K, Masumori N, Takahashi A, Itoh N, Kato K, Matusik RJ, Tsukamoto T. Murine androgen-independent neuroendocrine carcinoma promotes metastasis of human prostate cancer cell line LNCaP. Prostate 2006;66(5):536–545.
11. Saad F, Gleason DM, Murray R, Tchekmedyian S, Venner P, Lacombe L, Chin JL, Vinholes JJ, Goas JA, Chen B. A randomized, placebo-controlled trial of zoledronic acid in patients with hormone-refractory metastatic prostate carcinoma. J Natl Cancer Inst 2002;94(19):1458–1468.
12. Caraglia M, Marra M, Leonetti C, Meo G, D'Alessandro AM, Baldi A, Santini D, Tonini G, Bertieri R, Zupi G, Budillon A, Abbruzzese A. R115777 (Zarnestra)/Zoledronic acid (Zometa) cooperation on inhibition of prostate cancer proliferation is paralleled by Erk/Akt inactivation and reduced Bcl-2 and bad phosphorylation. J Cell Physiol 2007;211(2):533–543.
13. Patel YC. Somatostatin its receptor, family Front Neuroendocrinol 1999;20(3):157–198.
14. Hejna M, Schmidinger M, Raderer M. The clinical role of somatostatin analogs as antineoplastic agents: Much ado about nothing? Ann Oncol 2002;13(5):653–668.
15. Reubi JC, Waser B, Schaer JC, Laissue JA. Somatostatin receptor SSTR1–SSTR5 expression in normal and neoplastic human tissues using receptor autoradiography with subtype-selective ligands. Eur J Nucl Med 2001;28(7):836–846.
16. Halmos G, Schally AV, Sun B, Davis R, Bostwick DG, Plonowski A. High expression of somatostatin receptors and messenger ribonucleic acid for its receptor subtypes in organ-confined and locally advanced human prostate cancers. J Clin Endocrinol Metab 2000;85(7):2564–2571.
17. Bruns C, Lewis I, Briner U, Meno-Tetang G, Weckbecker G. SO M230 a novel somatostatin peptidomimetic with broad somatotropin release inhibiting factor (SRIF) receptor binding and a unique antisecretory profile. Eur J Endocrinol 2002 ;146(5):707–716.
18. Chou TC, Talalay P. Quantitative analysis of dose-effect relationships: The combined effects of multiple drugs or enzyme inhibitors. Adv Enzyme Regul 1984;22:27–55.
19. Topaly J, Zeller WJ, Fruehauf S. Synergistic activity of the new ABL-specific tyrosine kinase inhibitor STI571 and chemotherapeutic drugs on BCR-ABL-positive chronic myelogenous leukemia cells. Leukemia 2001;15(3):342–347.
20. Bok RA, Small EJ. Bloodborne biomolecular markers in prostate cancer development and progression. Nat Rev Cancer 2002;2(12):918–926.
21. Jin RJ, Wang Y, Masumori N, Ishii K, Tsukamoto T, Shappell SB, Hayward SW, Kasper S, Matusik RJ. NE-10 neuroendocrine cancer promotes the LNCaP xenograft growth in castrated mice. Cancer Res 2004;64(15):5489–5495.
22. Weinstein MH, Partin AW, Veltri RW, Epstein JI. Neuroendocrine differentiation in prostate cancer: Enhanced prediction of progression after radical prostatectomy. Hum Pathol 1996; 27(7):683–687.
23. Sciarra A, Bosman C, Monti G, Gentile V, Autran Gomez AM, Ciccariello M, Pastore A, Salvatori G, Fattore F, Di Silverio F. Somatostatin analogs and estrogens in the treatment of androgen ablation refractory prostate adenocarcinoma. J Urol 2004;172(5 Pt 1):1775–1783.
24. Pawlikowski M, Melen-Mucha G. Perspectives of new potential therapeutic applications of somatostatin analogs. Neuro Endocrinol Lett 2003;24(1–2):21–27.
25. van der Hoek J, van der Lelij AJ, Feelders RA, de Herder WW, Uitterlinden P, Poon KW, Boerlin V, Lewis I, Krahnke T, Hofland LJ, Lamberts SW. The somatostatin analogue SOM230, compared with octreotide, induces differential effects in several metabolic pathways in acromegalic patients. Clin Endocrinol (Oxf) 2005;63(2):176–184.
26. Schmid HA. Pasireotide (SOM230): Development, mechanism of action and potential applications. Mol Cell Endocrinol 2008;286(1–2):69–74.
27. Kavanagh KL, Guo K, Dunford JE, Wu X, Knapp S, Ebetino FH, Rogers MJ, Russell RG, Oppermann U. The molecular mechanism of nitrogen-containing bisphosphonates as antiosteoporosis drugs. Proc Natl Acad Sci USA 2006;103(20):7829–7834.
28. Hougland JL, Fierke CA. Getting a handle on protein prenylation. Nat Chem Biol 2009;5(4):197–198.
29. Nogawa M, Yuasa T, Kimura S, Kuroda J, Segawa H, Sato K, Yokota A, Koizumi M, Maekawa T. Zoledronic acid mediates Ras-independent growth inhibition of prostate cancer cells. Oncol Res 2005;15(1):1–9.
30. Fabbri F, Brigliadori G, Carloni S, Ulivi P, Vannini I, Tesei A, Silvestrini R, Amadori D, Zoli W. Zoledronic acid increases docetaxel cytotoxicity through pMEK and Mcl-1 inhibition in a hormone-sensitive prostate carcinoma cell line. J Transl Med 2008;6:43.
31. Mani J, Vallo S, Barth K, Makarevic J, Juengel E, Bartsch G, Wiesner C, Haferkamp A, Blaheta RA. Zoledronic acid influences growth, migration and invasive activity of prostate cancer cells in vitro. Prostate Cancer Prostatic Dis 2012;15(3):250–255.
32. Denoyelle C, Hong L, Vannier JP, Soria J, Soria C. New insights into the actions of bisphosphonate zoledronic acid in breast cancer cells by dual RhoA-dependent and -independent effects. Br J Cancer 2003;88(10):1631–1640.
33. Ottewell PD, Lefley DV, Cross SS, Evans CA, Coleman RE, Holen I. Sustained inhibition of tumor growth and prolonged survival following sequential administration of doxorubicin and zoledronic acid in a breast cancer model. Int J Cancer 2009;126(2):522–532.
34. Guenther A, Gordon S, Tiemann M, Burger R, Bakker F, Green JR, Baum W, Roelofs AJ, Rogers MJ, Gramatzki M. The bisphosphonate zoledronic acid has antimyeloma activity in vivo by inhibition of protein prenylation. Int J Cancer 2010;126(1):239–246.
35. Sewing L, Steinberg F, Schmidt H, Goke R. The bisphosphonate zoledronic acid inhibits the growth of HCT-116 colon carcinoma cells and induces tumor cell apoptosis. Apoptosis 2008; 13(6):782–789.
36. Tannehill-Gregg SH, Levine AL, Nadella MV, Iguchi H, Rosol TJ. The effect of zoledronic acid and osteoprotegerin on growth of human lung cancer in the tibias of nude mice. Clin Exp Metast 2006;23(1):19–31.
37. Kubista B, Trieb K, Sevelda F, Toma C, Arrich F, Heffeter P, Elbling L, Sutterluty H, Scotlandi K, Kotz R, Micksche M, Berger W. Anticancer effects of zoledronic acid against human osteosarcoma cells. J Orthop Res 2006;24(6):1145–1152.
38. Kuroda J, Kimura S, Segawa H, Kobayashi Y, Yoshikawa T, Urasaki Y, Ueda T, Enjo F, Tokuda H, Ottmann OG, Maekawa T. The third-generation bisphosphonate zoledronate synergistically augments the anti-pH + leukemia activity of imatinib mesylate. Blood 2003;102(6):2229–2235.
39. Hiraga T, Williams PJ, Ueda A, Tamura D, Yoneda T. Zoledronic acid inhibits visceral metastases in the 4T1/Luc mouse breast cancer model. Clin Cancer Res 2004;10(13):4559–4567.

40. Coxon JP, Oades GM, Kirby RS, Colston KW. Zoledronic acid induces apoptosis and inhibits adhesion to mineralized matrix in prostate cancer cells via inhibition of protein prenylation. BJU Int 2004;94(1):164–170.
41. Marten A, Lilienfeld-Toal M, Buchler MW, Schmidt J. Zoledronic acid has direct antiproliferative and antimetastatic effect on pancreatic carcinoma cells and acts as an antigen for delta2 gamma/delta T cells. J Immunother 2007;30(4):370–377.
42. Sato K, Kimura S, Segawa H, Yokota A, Matsumoto S, Kuroda J, Nogawa M, Yuasa T, Kiyono Y, Wada H, Maekawa T. Cytotoxic effects of gammadelta T cells expanded ex vivo by a third generation bisphosphonate for cancer immunotherapy. Int J Cancer 2005;116(1):94–99.
43. Roelofs AJ, Jauhiainen M, Monkkonen H, Rogers MJ, Monkkonen J, Thompson K. Peripheral blood monocytes are responsible for gamma delta T cell activation induced by zoledronic acid through accumulation of IPP/DMAPP. Br J Haematol 2009;144(2):245–250.
44. Reid IR, Brown JP, Burckhardt P, Horowitz Z, Richardson P, Trechsel U, Widmer A, Devogelaer JP, Kaufman JM, Jaeger P, Body JJ, Brandi ML, Broell J, Di Micco R, Genazzani AR, Felsenberg D, Happ J, Hooper MJ, Ittner J, Leb G, Mallmin H, Murray T, Ortolani S, Rubinacci A, Saaf M, Samsioe G, Verbruggen L, Meunier PJ. Intravenous zoledronic acid in postmenopausal women with low bone mineral density. N Engl J Med 2002;346(9):653–661.

World J Surg (2013) 37:1379–1387
DOI 10.1007/s00268-013-1989-6

World Journal of Surgery

Prognosis and Predictors of Surgical Complications in Hepatocellular Carcinoma Patients With or Without Cirrhosis after Hepatectomy

Toru Mizuguchi · Masaki Kawamoto · Makoto Meguro · Yukio Nakamura · Shigenori Ota · Thomas T. Hui · Koichi Hirata

Published online: 12 March 2013

Abstract
Background Although poor liver function is associated with a high morbidity rate and poor prognosis in hepatocellular carcinoma (HCC) patients, the exact effects of liver pathology on the surgical outcomes of HCC patients are poorly understood. The purpose of this study was to assess how the liver pathology of HCC patients affects their prognosis and complications rate after liver resection.
Methods Between January 2006 and November 2010, 149 consecutive hepatocellular carcinoma patients, including 79 noncirrhosis patients and 70 cirrhosis patients, were enrolled in this study.
Results Among the noncirrhotic patients, operative time, fresh frozen plasma (FFP) transfusion requirement, tumor size, and serum retinol binding protein (RBP) levels were significantly higher in the complications group than in the complications-free groups. On the other hand, in the cirrhotic patients the prothrombin time (PT) and indocyanine green retention value at 15 min ($ICGR_{15}$) of the complications group were significantly lower and higher, respectively, than those of the complications-free group. In the noncirrhotic patients, recurrence-free survival and overall survival did not differ between the complications and complications-free groups. On the other hand, in the cirrhotic patients, the recurrence-free survival and overall survival of the complications-free group were significantly longer than those of the complications group.
Conclusions In the noncirrhotic patients, surgical complications had no prognostic effect, whereas they had a significant survival impact in the cirrhotic patients. The surgical strategy for HCC should be based on the patient's pathological background.

T. Mizuguchi (✉) · M. Kawamoto · M. Meguro · Y. Nakamura · S. Ota · K. Hirata
Department of Surgery I, Sapporo Medical University Hospital, Sapporo Medical University School of Medicine, S-1, W-16, Chuo-Ku, Sapporo, Hokkaido 060-8543, Japan
e-mail: tmizu@sapmed.ac.jp

T. T. Hui
Department of Surgery, Children's Hospital & Research Center Oakland, 747 52nd Street, Oakland, CA 94609, USA

Introduction

Hepatocellular carcinoma (HCC) is the sixth most prevalent cancer worldwide and the third most common cause of cancer-related death [1, 2]. The optimal management strategy for HCC depends on both tumor-related factors and host liver function [3, 4]. Although the frequency of nonalcoholic steatohepatitis-related HCC has recently increased [5, 6], most HCC still develops in patients with viral hepatitis-associated liver disease [1, 2]. In the era when no effective viral therapy was available, a high incidence of recurrence after treatment was inevitable in HCC patients. Therefore, surgery for HCC tended to be avoided in patients with good liver function [7]. In addition, the high mortality rate of liver resection itself encouraged patients and doctors to select interventional therapy instead of a surgical approach.

However, liver surgery techniques have improved, and the mortality rate after liver resection was nearly zero in recent cases [8, 9]. In addition, technical developments have encouraged surgeons to select a laparoscopic approach instead of conventional open surgery [10, 11]. In liver resection for HCC, the current goal is to reduce the morbidity rate as much as possible and improve patient prognosis. Liver transplantation is considered to be the best curative approach for HCC, but liver resection should be

considered in cases in which it would be expected to achieve a good prognosis [9, 12]. Furthermore, the mortality rate of liver resection is lower than that of liver transplantation in the early stages of HCC, and among patients with good liver function the long-term prognosis of patients who undergo liver resection is comparable to that of patients that undergo liver transplantation [9].

Although poor liver function is associated with a high morbidity rate and poor prognosis in HCC patients [13, 14], the exact effects of liver pathology on the surgical outcomes of HCC patients are poorly understood. Therefore, the purpose of this study was to identify how liver pathology affected the prognosis and complications rates of consecutive HCC patients who underwent liver resection.

Patients and methods

Between January 2006 and November 2010, 149 consecutive hepatocellular carcinoma patients who underwent hepatectomy were enrolled in this study after providing informed consent. Mortality was defined as any in-hospital death that occurred within 90 days of surgery. Postoperative complications were defined and classified according to the modified Clavien classification system [15]. Briefly, Grade I complications were defined as any deviation from the normal postoperative course that did not require special treatment. Grade II complications were defined as those that required pharmacological treatment with drugs. Grade III complications were defined as those that required surgical or radiological intervention with (IIIb) or without (IIIa) general anesthesia. Grade IV complications were defined as life-threatening complications involving single (IVa) or multiple (IVb) organ dysfunction. Grade V complications were defined as those that caused the death of the patient. For grade IV or worse complications, liver failure was defined as a serum bilirubin concentration of greater than 5 mg/dl that lasted for more than 2 days. Renal dysfunction/insufficiency was defined as oliguria (<400 ml/day) combined with a sustained serum creatine level elevation of more than 1.1 mg/dl. Bleeding was diagnosed by endoscopic examination. Wound seroma/infection was defined as any wound that split open regardless of whether bacteria were detected. Ascites was defined as fluid discharge of more than 300 ml/day for more than 3 days.

We divided the patients into two groups: the noncirrhosis group (79 patients) and the cirrhosis group (70 patients). The study design conformed to the ethical guidelines of the Declaration of Helsinki, and obtained informed consent was obtained from each subject before their registration.

Assessment of clinical and operative variables

Before hepatectomy, we performed laboratory tests to assess the patients' serum levels of type IV collagen (Col), hyaluronic acid (HA), prealbumin (PreALB), retinol binding protein (RBP), hepatocyte growth factor (HGF), alpha fetoprotein (AFP), and protein induced by vitamin K absence or antagonists-II (PIVKAII), as well as their indocyanine green retention value at 15 min ($ICGR_{15}$) and ^{99}m-technetium-labeled galactosyl serum albumin (GSA) scintigraphy index (HH15, LHL15) values. Their intraoperative data and any complications that occurred during hospitalization also were recorded. Tumor size and number were assessed by pathological examinations. All laboratory tests were conducted in the early morning on the day of assessment. The model for end-stage liver disease (MELD) score of each patient was calculated using the following formula: $9.57 \times \text{Ln}$ (creatinine mg/dL) $+ 3.78 \times \text{Ln}$ (bilirubin mg/dL) $+ 11.20 \times \text{Ln}$ (PT-INR) $+ 6.43$, based on laboratory tests [16].

The Child–Pugh score with Pugh's modification was calculated as the sum of the scores for five clinical parameters [ascites (none = one point, moderate = two points, severe = three points), serum bilirubin (<2 mg/dl = one point, 2–3 mg/dl = two points, >3 mg/dl = three points), serum albumin (>3.5 g/dl = one point, 2.8–3.5 g/dl = two points, <2.8 g/dl = three points), hepatic encephalopathy (absent = one point, grade 1 or 2 = two points, grade 3 or 4 = three points), and prothrombin index [>70 % = one point, 40–70 % = two points, <40 % = three points]). Then, the patients were classified into three groups with different expected survivals according to their Child–Pugh scores (Child–Pugh A = 5–6 points, Child–Pugh B = 7–9 points, Child–Pugh C = 10 or more points) [17].

Surgical procedure

All liver resections were performed with the Pringle maneuver after more than 300 ml of intraoperative bleeding. Hepatic flow was not controlled if the intraoperative bleeding was less than 300 ml. A Cavitron ultrasonic aspirator (CUSA) was used for liver parenchymal dissection, and an argon laser beam coagulator or saline-associated monopolar electrocautery was used to achieve hemostasis. Antibiotics were administered 30 min before the laparotomy and every 3 h during the operation. All of the sutures and ties, except those used for skin closure, were absorbable (Vicryl or PDS, Johnson & Johnson Gateway, Piscataway, NJ). The periwound skin was washed with 500 ml of warm saline before skin closure. A closed-type intra-abdominal drain and a subcutaneous drain were installed for 2–3 days after the liver resection.

The operation type was classified as follows: hepatic resection (Hr) 0: partial resection including tumor enucleation; Hr S: sub-segmentectomy; Hr 1: mono-segmentectomy; Hr 2: bi-segmentectomy including right hepatectomy, left hepatectomy, and central bi-segmentectomy; and Hr 3: tri-segmentectomy.

Statistical analysis

For the statistical analyses, demographic data and perioperative laboratory test results were extracted from the clinical database, and the differences among the groups were compared using the χ^2 test followed by the post-hoc 2×2 Fisher's exact test, when necessary. Continuous variables were compared using the Mann–Whitney U test. Logistic regression analysis was used to identify the most relevant risk factors for complications. The factors affecting overall survival were assessed using the Kaplan–Meier method, with comparisons performed using the log-rank test and univariate or multivariate analyses performed using the Cox proportional hazards regression model. All calculations were performed using the StatView 5.0 software package (Abacus Concepts Inc., Berkeley, CA) or SPSS 16.0 (SPSS Inc., Chicago, IL). Receiver operating characteristic (ROC) curves, which were used to calculate the area under the ROC curve (AUC), were produced using the MedCalc software package (Ver 8.0.1.0, Mariakerke, Belgium). All results are expressed as median values (minimum value-maximum value). P values <0.05 were considered to be statistically significant.

Results

Of the 149 consecutive patients in which we performed hepatectomy for HCC, postoperative pathological liver evaluations found that 79 patients had noncirrhotic livers, and 70 patients had cirrhotic livers. The two groups displayed similar morbidity rates, and there were no significant differences in the frequencies of any of the complications included in the Clavien classification (Table 1).

Table 2 shows the clinical demographics of the noncirrhotic patients. In univariate analysis of these patients, the operative time, fresh frozen plasma (FFP) transfusion requirement, tumor size, MELD score, and γ-glutamyl transpeptidase (gGT), and retinol binding protein (RBP) levels of the complications group were found to be significantly higher than those of the complications-free group. Multivariate analysis demonstrated that all of these indicators, except gGT and the MELD score, were significantly increased in the complications group. The area under the curve (AUC) values of these indicators were all greater than 0.65 and were significantly different (Fig. 1a–d). Interactive dot diagrams were used to determine the ideal cutoff values for each parameter, which were 3.1 mg/dl for RBP (Fig. 1e), 373 min for operative time (Fig. 1f), 0 U for FFP transfusion requirement (Fig. 1g), and 5.5 cm for tumor size (Fig. 1h).

Table 1 Postoperative complications suffered by noncirrhotic and cirrhotic patients after hepatectomy for hepatocellular carcinoma

Clavien classification	Noncirrhotic ($n = 79$)		Cirrhotic ($n = 70$)	
	GI–GIII	GIV–GV	GI–GIII	IV–GV
Liver failure	1	1	1	1
Bleeding	1		2	
Bile leakage	3		1	
Respiratory distress	5		1	1
Renal dysfunction/failure	2		2	
Intra-abdominal abscess	3		2	
Wound seroma/infection	5		3	
Pleural effusion	3		5	
Ascites	3		10	
	28 events/ 22 patients		29 events/ 24 patients	

Table 3 shows the clinical demographics of the cirrhotic patients. In univariate analysis of these patients, the prothrombin time (PT), choline esterase (CholE) levels, Child–Pugh score, and MELD score of the complications group were found to be significantly higher than those of the complications-free group, whereas the indocyanine green retention value at 15 min ($ICGR_{15}$) of the complications group was significantly lower than that of the complications-free group. Of these, PT and the $ICGR_{15}$ achieved significance in the multivariate analysis. The AUC values of both of these parameters were greater than 0.65 and were significantly different (Fig. 2a, b). Interactive dot diagrams demonstrated the ideal cutoff values for each of these parameters, which were 82.8 % for PT (Fig. 2c) and 9.6 % for the $ICGR_{15}$ (Fig. 2d).

We next examined the recurrence-free survival (Fig. 3a, c) and overall survival (Fig. 3b, d) rates of the noncirrhotic (Fig. 3a, b) and cirrhotic patients (Fig. 3c, d). Among the non-cirrhotic patients, the complications and complications-free groups displayed similar recurrence-free survival and overall survival rates. On the other hand, among the cirrhotic patients, the complications-free group demonstrated significantly longer recurrence-free survival and overall survival than the complications group.

Discussion

In this study, we showed that the risk factors for perioperative complications differed between noncirrhotic

Table 2 Clinical demographics of the noncirrhotic patients who underwent initial hepatectomy for hepatocellular carcinoma ($N = 79$)

	Complications	Complications-free	Univariate	Multivariate
Etiology			0.262	
B	8	25		
C	6	20		
BC	1	0		
NBNC	7	12		
Operation			0.054	
0	5	24		
S	3	13		
1	6	11		
2	4	8		
3	4	1		
Stage			0.678	
1	1	8		
2	16	32		
3	3	10		
4	2	7		
Operative time (min)	415.6 ± 143.9	332.7 ± 134.8	0.019	0.043
Bleeding (ml)	857.8 ± 609.3	552.4 ± 1261.1	0.282	
Blood transfusion (U)	1.9 ± 3.2	0.6 ± 2.4	0.053	
FFP transfusion (U)	4.0 ± 6.1	1.1 ± 3.1	0.006	0.001
Tumor size (cm)	6.62 ± 4.06	4.22 ± 3.14	0.009	0.001
Tumor number	1.6 ± 1.2	1.6 ± 1.5	0.979	
Age (year)	67.7 ± 9.2	67.9 ± 11.2	0.931	
Height (cm)	161.9 ± 7.6	160.5 ± 7.5	0.463	
Weight (kg)	61.4 ± 10.2	58.7 ± 9.8	0.289	
BMI	23.5 ± 3.1	22.7 ± 3.2	0.307	
ALB (g/dl)	3.81 ± 0.53	3.93 ± 0.35	0.252	
Bil (mg/dl)	0.61 ± 0.34	0.72 ± 0.34	0.189	
PT (%)	92.9 ± 9.4	92.8 ± 13.5	0.979	
Plt ($\times 10^4$)	18.2 ± 6.8	17.7 ± 11.5	0.844	
AT (%)	96.9 ± 16.8	94.4 ± 17.2	0.577	
AST (IU/L)	43.4 ± 25.6	38.8 ± 39.4	0.617	
ALT (IU/L)	41.4 ± 29.7	36.4 ± 30.9	0.516	
gGT (IU/L)	117.2 ± 180.6	52.7 ± 47.1	0.022	0.056
CholE (IU/L)	245.3 ± 79.1	250.4 ± 66.1	0.776	
Col (ng/ml)	5.52 ± 2.83	4.99 ± 1.46	0.322	
HA (ng/ml)	160.1 ± 143.5	141.6 ± 207.1	0.712	
BTR	6.49 ± 2.21	6.53 ± 1.79	0.941	
ICG R15 (%)	10.1 ± 8.5	10.8 ± 6.7	0.692	
RBP (mg/dl)	4.47 ± 3.68	2.68 ± 1.13	0.005	0.024
PreALB (mg/dl)	21.3 ± 8.1	18.8 ± 6.6	0.195	
HGF (ng/ml)	0.34 ± 0.11	0.29 ± 0.13	0.199	
HH15	0.602 ± 0.062	0.584 ± 0.069	0.299	
LHL15	0.930 ± 0.027	0.933 ± 0.029	0.675	
Child–Pugh score	5.318 ± 0.477	5.281 ± 0.701	0.818	
MELD score	8.901 ± 5.314	7.402 ± 1.156	0.046	0.095

patients and cirrhotic patients who had undergone liver resection for HCC. In addition, the effects of surgical complications on postoperative recurrence-free survival and overall survival also differed among these groups. These results indicate that the pathological state of the patient's liver should be taken into account when

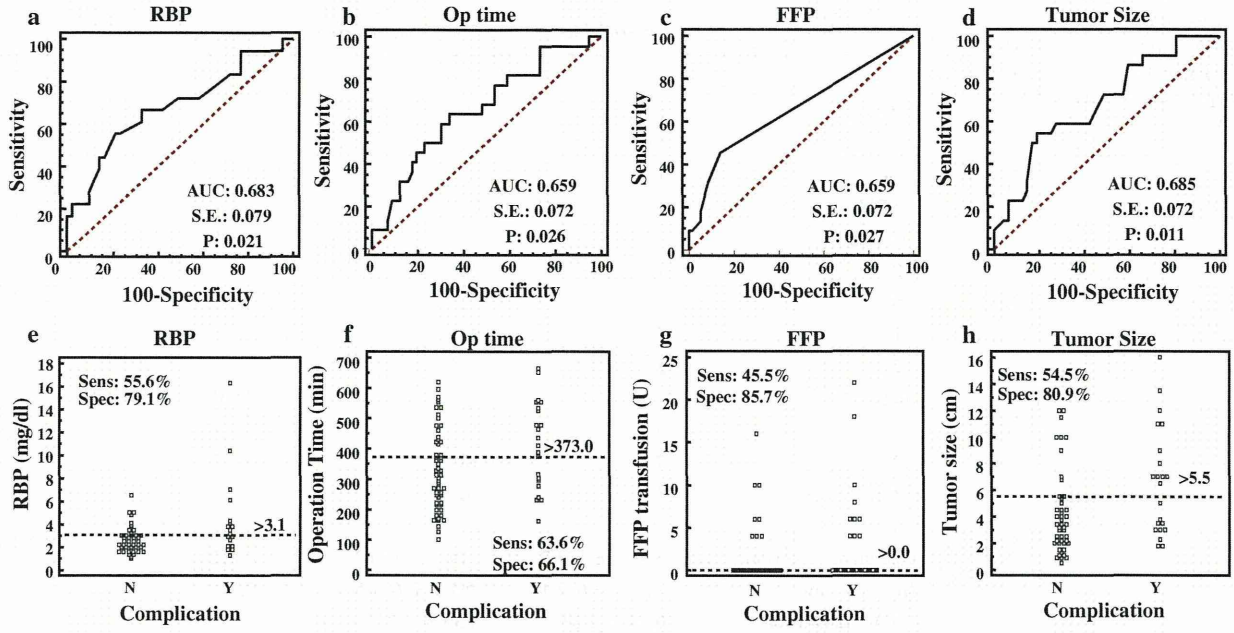

Fig. 1 ROC curves (**a, b, c,** and **d**) and interactive dot diagrams (**e, f, g,** and **h**) of retinol binding protein levels (RBP; **a** and **e**), operative time (Op time; **b** and **f**), fresh frozen plasma transfusion requirement (FFP; **c** and **g**), and tumor size (**d** and **h**). *AUC* area under the ROC curve, *SE* standard error, *CI* confidence interval, *Sens.* sensitivity, *Spec.* specificity, *N* no, *Y* yes. $P < 0.05$ was considered to be significant

determining the optimal surgical management strategy for HCC or predicting the prognosis of HCC patients.

The risk factors for surgical complications in HCC patients can be divided into technical and host factors [13, 14, 18–21]. We did not detect any difference in the frequency of surgical complications between the non-cirrhotic and cirrhotic patients, even though they displayed different risk factors. The extent of liver resection tended to be greater in the noncirrhotic patients, which might have increased their risk of surgical complications. On the other hand, only limited liver resection can be performed in cirrhotic patients due to their poor liver function. Although cirrhotic patients are expected to display a higher risk of surgical complications than noncirrhotic patients due to their immunocompromised condition [18, 21], the limited resections performed in cirrhotic patients might counteract this effect [22]. Another possible reason for the similar complication rates of the two groups is that we might not have performed the operations involving the noncirrhotic patients with sufficient technical skill as the tumors in the complications group were larger than those in the complications-free group, which would have made the procedures more technically difficult. We did not fully elucidate the reason why the noncirrhotic and cirrhotic patients displayed similar complication rates, but we might have to reconsider our surgical management strategy for noncirrhotic patients.

In the noncirrhotic patients, the serum RBP level was found to be a predictive risk factor for surgical complications in addition to tumor size and operative time. Patients' preoperative hepatic reserves are usually evaluated using the Child–Pugh score or liver damage score [3, 23–26]. A previous study found that in noncirrhotic patients these classical liver functional evaluation methods gave similar results for each patient, and it was hard to distinguish between borderline cases [7]. Due to the short half-life of RBP, its serum concentration represents the real-time state of hepatic protein production [23, 27]. In fact, our results suggested that serum RBP levels could be a useful predictor of surgical complications. Therefore, serum RBP levels could be used to predict postoperative complications and determine the hepatic condition of noncirrhotic patients.

Among the noncirrhotic patients, the complications and complications-free groups displayed similar prognoses. The tumors in the complications group were larger than those in the complications-free group, although the two groups displayed similar numbers of tumors. Tumor size and number have been reported to be prognostic factors for HCC patients [3]. However, many of the patients in the complications group had large single tumors. It is possible that tumor size does not have a prognostic impact in cases involving single tumors, but rather, only has a clinical impact in terms of the technical difficulties associated with large tumors. In fact, Truant recently reported that in HCC

Table 3 Clinical demographics of the cirrhotic patients who underwent hepatectomy for hepatocellular carcinoma ($N = 70$)

	Complications	Complications-free	Univariate	Multivariate
Etiology			0.137	
B	9	20		
C	11	22		
BC	1	2		
NBNC	3	2		
Operation			0.339	
0	12	22		
S	4	12		
1	5	9		
2	3	3		
Stage			0.856	
1	6	10		
2	7	18		
3	10	16		
4	1	2		
Operative time (min)	376.7 ± 133.7	319.7 ± 130.2	0.092	
Bleeding (ml)	718.5 ± 677.1	461.9 ± 621.5	0.119	
Blood transfusion (U)	0.83 ± 2.63	0.35 ± 1.31	0.317	
FFP transfusion (U)	3.26 ± 4.33	1.49 ± 4.28	0.115	
Tumor size (cm)	3.28 ± 1.91	2.69 ± 1.46	0.192	
Tumor number	2.4 ± 3.4	1.5 ± 0.9	0.137	
Age (year)	66.5 ± 8.9	65.6 ± 10.3	0.733	
Height (cm)	160.7 ± 8.9	159.4 ± 9.5	0.576	
Weight (kg)	62.4 ± 11.1	60.4 ± 12.2	0.501	
BMI	24.1 ± 3.2	23.7 ± 3.5	0.657	
ALB (g/dl)	3.63 ± 0.39	3.82 ± 0.61	0.174	
Bil (mg/dl)	0.84 ± 0.49	0.74 ± 0.31	0.291	
PT (%)	83.9 ± 10.3	89.9 ± 8.7	0.019	0.007
Plt ($\times 10^4$)	14.2 ± 9.9	13.1 ± 8.3	0.596	
AT (%)	77.5 ± 14.8	82.1 ± 15.9	0.254	
AST (IU/L)	46.8 ± 20.4	47.6 ± 21.5	0.881	
ALT (IU/L)	42.9 ± 25.7	44.2 ± 26.1	0.838	
gGT (IU/L)	94.8 ± 72.5	77.9 ± 84.4	0.428	
CholE (IU/L)	195.3 ± 63.4	236.6 ± 65.7	0.019	0.091
Col (ng/ml)	7.44 ± 2.64	6.53 ± 2.34	0.179	
HA (ng/ml)	270.5 ± 203.3	211.4 ± 157.1	0.189	
BTR	5.22 ± 2.14	5.51 ± 2.32	0.639	
$ICGR_{15}$ (%)	17.4 ± 7.7	12.3 ± 7.3	0.011	0.022
RBP (mg/dl)	2.31 ± 1.22	2.65 ± 1.55	0.392	
PreALB (mg/dl)	14.9 ± 4.9	17.1 ± 7.1	0.194	
HGF (ng/ml)	0.47 ± 0.15	0.42 ± 0.22	0.331	
HH15	0.669 ± 0.101	0.624 ± 0.087	0.069	
LHL15	0.889 ± 0.071	0.911 ± 0.045	0.144	
Child–Pugh score	5.542 ± 0.779	5.222 ± 0.421	0.029	0.182
MELD score	8.595 ± 1.888	7.683 ± 1.374	0.025	0.097

large tumors were associated with a worse prognosis, but some patients whose tumors were not very aggressive achieved better survival regardless of the size of their tumor [28]. Regardless of how tumor size is related to prognosis, surgical complications do not have a prognostic impact in non-cirrhotic patients.

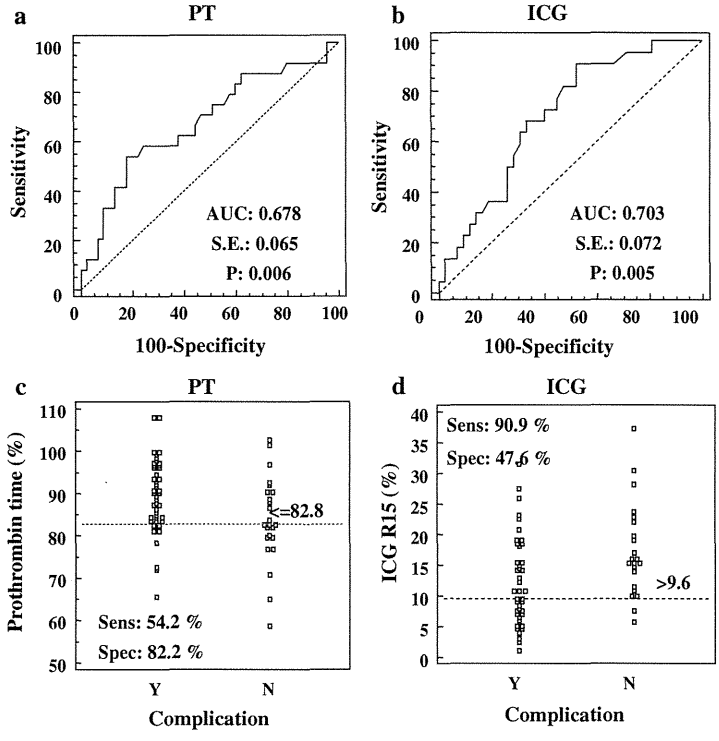

Fig. 2 ROC curves (**a** and **b**) and interactive dot diagrams (**c** and **d**) of prothrombin time (PT; **a** and **c**) and the indocyanine green retention value at 15 min ($ICGR_{15}$; **b** and **d**). *AUC* area under the ROC curve, *SE* standard error, *CI* confidence interval, *Sens.* sensitivity, *Spec.* specificity, *N* no, *Y* yes. $P < 0.05$ was considered to be significant

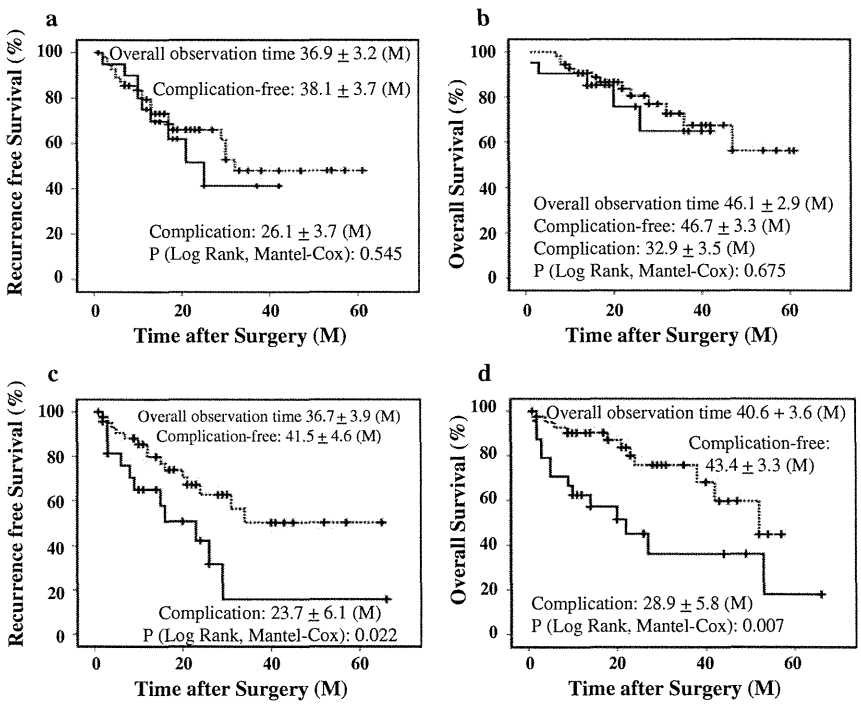

Fig. 3 Recurrence-free survival (**a** and **c**) and overall survival (**b** and **d**) in the noncirrhotic patients (**a** and **b**) and cirrhotic patients (**c** and **d**). *Straight lines* represent the complications group, and *dotted lines* represent the complications-free group

In the cirrhotic patients, PT and the $ICGR_{15}$ were found to be predictors of surgical complications. Although the $ICGR_{15}$ does not count towards the Child–Pugh score, the liver damage score consists of serum albumin and bilirubin levels, PT, and the $ICGR_{15}$ [23, 24]. Thus, our study showed that liver function has a prognostic impact in

cirrhotic patients, as was found in previous reports [14], whereas postoperative complications had no prognostic effect in noncirrhotic patients. Our finding that liver function had a significant impact on postoperative complications in cirrhotic patients has important implications. We found that PT and $ICGR_{15}$ cutoff levels of 80 and 10 %, respectively, can be used to predict which patients will suffer surgical complications and a poor prognosis. Our cutoff values are very similar to those used for the liver damage score. Thus, although the risk of complications is affected by the extent of tumor progression and the type of liver resection in noncirrhotic patients, classical functional evaluations of liver function, such as the Child–Pugh score [17] or liver damage score, are helpful not only for determining surgical indications but also for predicting postoperative complications and prognosis, especially in cirrhotic patients.

On the other hand, the MELD score has been shown to be a predictor of liver failure in cirrhotic patients [29]. However, the MELD score did not achieve statistical significance in the multivariate analysis conducted in the present study. This might have been due to the surgical indications for HCC employed at our institution. Basically, decompensated cirrhotic patients are never considered for liver resection. In addition, there were no patients with hepatorenal syndrome, and most of the patients' serum bilirubin levels were within normal levels. Therefore, the MELD score was dependent on the PT-INR in most patients. Although consecutive studies might be subject to inevitable bias, PT-related scores, including PT itself, might be useful for predicting complications and prognosis in cirrhotic patients.

The morbidity rates of the noncirrhotic patients and cirrhotic patients in our study were not significantly different. The most common complications suffered by the noncirrhotic patients were bile leakage, bleeding, and surgical site infections, including intra-abdominal abscesses and wound infection. On the other hand, the most common complications experienced by the cirrhotic patients were ascites and pleural effusion. The fact that the operations performed in the noncirrhotic patients involved more extensive resections than those performed in the cirrhotic patients, which also affected the resected liver area and wound length, might have caused these responsible these differences. On the other hand, morbidity is inevitable in cirrhotic patients due to their poor systemic condition, which is caused by their poor liver function [7, 14]. The risk of morbidity after liver resection depends on the balance between liver function and operative procedure. Therefore, we need to pay more attention to the surgical management of noncirrhotic patients and the surgical indications and operative plans for cirrhotic patients.

Conclusions

We investigated the predictors of surgical complications after liver resection for HCC according to the pathological background of the patient's liver. In noncirrhotic patients, serum RBP level, tumor size, operation time, and FFP transfusion requirement were found to be predictors of surgical complications, although surgical complications had no prognostic impact in this group. On the other hand, PT and the $ICGR_{15}$ were found to be predictors of surgical complications in the cirrhotic patients, and surgical complications conveyed a significant survival disadvantage in this group.

Surgical strategies for HCC should take the patient's pathological background into account.

Acknowledgments The authors thank Daniel Mrozek (Medical English Service, Kyoto, Japan) for his help preparing this manuscript. Part of this study was supported by a Grant-in-Aid for Scientific Research from the Ministry of Education, Culture, Sports, Science, and Technology (No. 23591993) and a Grant from the Yuasa Memorial Foundation to T. Mizuguchi.

Conflict of interest None

References

1. Forner A, Llovet JM, Bruix J (2012) Hepatocellular carcinoma. Lancet 379:1245–1255
2. El-Serag HB (2012) Epidemiology of viral hepatitis and hepatocellular carcinoma. Gastroenterology 142:1264–1273
3. Vauthey JN, Dixon E, Abdalla EK et al (2010) Pretreatment assessment of hepatocellular carcinoma: expert consensus statement. HPB (Oxford) 12:289–299
4. Chow PK (2012) Resection for hepatocellular carcinoma: is it justifiable to restrict this. to the American Association for the Study of the Liver/Barcelona Clinic for Liver Cancer criteria? J Gastroenterol Hepatol 27:452–457
5. Starley BQ, Calcagno CJ, Harrison SA (2010) Nonalcoholic fatty liver disease and hepatocellular carcinoma: a weighty connection. Hepatology 51:1820–1832
6. Reddy SK, Steel JL, Chen HW et al (2012) Outcomes of curative treatment for hepatocellular cancer in nonalcoholic steatohepatitis versus hepatitis C and alcoholic liver disease. Hepatology 55:1809–1819
7. Mizuguchi T, Katsuramaki T, Nobuoka T et al (2004) Serum hyaluronate level for predicting subclinical liver dysfunction after hepatectomy. World J Surg 28:971–976. doi:10.1007/s00268-004-7389-1
8. Takayama T (2011) Surgical treatment for hepatocellular carcinoma. Jpn J Clin Oncol 41:447–454
9. Rahbari NN, Mehrabi A, Mollberg NM et al (2011) Hepatocellular carcinoma: current management and perspectives for the future. Ann Surg 253:453–469
10. Bryant R, Laurent A, Tayar C et al (2009) Laparoscopic liver resection-understanding its role in current practice: the Henri Mondor Hospital experience. Ann Surg 250:103–111
11. Reddy SK, Tsung A, Geller DA (2011) Laparoscopic liver resection. World J Surg 35:1478–1486. doi:10.1007/s00268-010-0906-5

12. Koniaris LG, Levi DM, Pedroso FE et al (2011) Is surgical resection superior to transplantation in the treatment of hepatocellular carcinoma? Ann Surg 254:527–537
13. Chok KS, Ng KK, Poon RT et al (2009) Impact of postoperative complications on long-term outcome of curative resection for hepatocellular carcinoma. Br J Surg 96:81–87
14. Mizuguchi T, Nagayama M, Meguro M et al (2009) Prognostic impact of surgical complications and preoperative serum hepatocyte growth factor in hepatocellular carcinoma patients after initial hepatectomy. J Gastrointest Surg 13:325–333
15. Dindo D, Demartines N, Clavien PA (2004) Classification of surgical complications: a new proposal with evaluation in a cohort of 6336 patients and results of a survey. Ann Surg 240: 205–213
16. Kamath PS, Wiesner RH, Malinchoc M et al (2001) A model to predict survival in patients with end-stage liver disease. Hepatology 33:464–470
17. Pugh RN, Murray-Lyon IM, Dawson JL et al (1973) Transection of the oesophagus for bleeding oesophageal varices. Br J Surg 60:646–649
18. Benzoni E, Cojutti A, Lorenzin D et al (2007) Liver resective surgery: a multivariate analysis of postoperative outcome and complication. Langenbecks Arch Surg 392:45–54
19. Yang T, Zhang J, Lu JH et al (2011) Risk factors influencing postoperative outcomes of major hepatic resection of hepatocellular carcinoma for patients with underlying liver diseases. World J Surg 35:2073–2082. doi:10.1007/s00268-011-1161-0
20. Okamura Y, Takeda S, Fujii T et al (2011) Prognostic significance of postoperative complications after hepatectomy for hepatocellular carcinoma. J Surg Oncol 104:814–821
21. Young AL, Adair R, Prasad KR et al (2012) Hepatocellular carcinoma within a noncirrhotic, nonfibrotic, seronegative liver: surgical approaches and outcomes. J Am Coll Surg 214:174–183
22. Belli G, Fantini C, D'Agostino A et al (2004) Laparoscopic liver resections for hepatocellular carcinoma (HCC) in cirrhotic patients. HPB (Oxford) 6:236–246
23. Schneider PD (2004) Preoperative assessment of liver function. Surg Clin North Am 84:355–373
24. Hasegawa K, Kokudo N (2009) Surgical treatment of hepatocellular carcinoma. Surg Today 39:833–843
25. Manizate F, Hiotis SP, Labow D et al (2010) Liver functional reserve estimation: state of the art and relevance to local treatments. Oncology 78(Suppl 1):131–134
26. Mizuguchi T, Kawamoto M, Meguro M et al (2012) Serum antithrombin III level is well correlated with multiple indicators for assessment of liver function and diagnostic accuracy for predicting postoperative liver failure in hepatocellular carcinoma patients. Hepatogastroenterology 59:551–557
27. Goodman DS (1980) Plasma retinol-binding protein. Ann NY Acad Sci 348:378–390
28. Truant S, Boleslawski E, Duhamel A et al (2012) Tumor size of hepatocellular carcinoma in noncirrhotic liver: a controversial predictive factor for outcome after resection. Eur J Surg Oncol 38:1189–1196
29. Cucchetti A, Ercolani G, Vivarelli M et al (2006) Impact of model for end-stage liver disease (MELD) score on prognosis after hepatectomy for hepatocellular carcinoma on cirrhosis. Liver Transpl 12:966–971

Cancer Chemother Pharmacol (2013) 71:789–797
DOI 10.1007/s00280-013-2073-5

ORIGINAL ARTICLE

A phase II study of neoadjuvant combination chemotherapy with docetaxel, cisplatin, and S-1 for locally advanced resectable gastric cancer: nucleotide excision repair (NER) as potential chemoresistance marker

Masahiro Hirakawa · Yasushi Sato · Hiroyuki Ohnuma · Tetsuji Takayama · Tamotsu Sagawa · Takayuki Nobuoka · Keisuke Harada · Hiroshi Miyamoto · Yasuhiro Sato · Yasuo Takahashi · Shinich Katsuki · Michiaki Hirayama · Minoru Takahashi · Michihiro Ono · Masahiro Maeda · Kohichi Takada · Tsuyoshi Hayashi · Tsutomu Sato · Koji Miyanishi · Rishu Takimoto · Masayoshi Kobune · Koichi Hirata · Junji Kato

Received: 9 October 2012 / Accepted: 31 December 2012 / Published online: 22 January 2013

Abstract
Purpose The combination of docetaxel, cisplatin, and S-1 (DCS) chemotherapy is expected to be a promising regimen for advanced gastric cancer. This study was performed to evaluate the efficacy and safety of neoadjuvant DCS chemotherapy for locally advanced resectable gastric cancer.
Methods Patients with locally advanced gastric cancer received 2 courses of preoperative chemotherapy with S-1 (40 mg/m^2 b.i.d.) on days 1–14 and docetaxel (60 mg/m^2) plus cisplatin (60 mg/m^2) on day 8 every 3 weeks, followed by standard curative surgery within 4–8 weeks. The primary endpoint was R0 resectability. Expression of damage DNA binding protein complex subunit 2 (DDB2)/excision repair cross-complementing 1 (ERCC1) in the pretreated tumor tissues was examined by immunohistochemistry.
Results A total of 43 patients received neoadjuvant chemotherapy. The response rate was 74.4 %, and disease control ratio was 100 %. Grade 4 neutropenia developed in 53.5 % of patients and febrile neutropenia in 16.3 %. Non-hematological grade 3/4 adverse events were anorexia (23.3 %), nausea (14.0 %), and diarrhea (23.3 %), but these were generally transient and manageable. The proportion of R0 resections in the 43 eligible patients was 90.7 %, and a pathological response was found in 65.9 % of patients. There were no treatment-related deaths and no major surgical complications. The accuracy of the

Masahiro Hirakawa and Yasushi Sato contributed equally to this work.

Trial registration ID: UMIN000000801.

M. Hirakawa · Y. Sato (✉) · H. Ohnuma · K. Takada · T. Hayashi · T. Sato · K. Miyanishi · R. Takimoto · M. Kobune · J. Kato
Fourth Department of Internal Medicine, Sapporo Medical University School of Medicine, South 1 West 16, Chuo-ku, Sapporo 060-8543, Japan
e-mail: yasushis@sapmed.ac.jp

T. Takayama · H. Miyamoto
Department of Gastroenterology and Oncology, Institute of Health Biosciences, The University of Tokushima Graduate School, Tokushima, Japan

T. Sagawa · Y. Sato · Y. Takahashi
Division of Gastroenterology, Hokkaido Cancer Center, Sapporo, Japan

T. Nobuoka · K. Harada · K. Hirata
First Department of Surgery, Sapporo Medical University School of Medicine, Sapporo, Japan

S. Katsuki
Division of Gastroenterology, Otaru Ekisaikai Hospital, Otaru, Japan

M. Hirayama
Division of Gastroenterology, Tonan Hospital, Sapporo, Japan

M. Takahashi
Division of Gastroenterology, Sapporo Kyoritsu Gorinbashi Hospital, Sapporo, Japan

M. Ono · M. Maeda
Division of Gastroenterology, Steel Memorial Muroran Hospital, Muroran, Japan

combination of DDB2 and ERCC1 expression for predicting chemoresistance was 82.5 %.
Conclusions Preoperative treatment with DCS combination for locally advanced gastric cancer demonstrated a sufficient R0 resection rate and a good pathological response with manageable toxicities. The DDB2/ERCC1-high phenotype, as determined by immunohistochemistry, may be useful predictor of resistance to DCS chemotherapy.

Keywords Neoadjuvant chemotherapy · Advanced resectable gastric cancer · DSC · Nucleotide excision repair

Introduction

Although the incidence of gastric cancer is decreasing, it remains the second leading cause of cancer-related death globally and in Japan [1]. A further decrease in mortality would require improved treatment outcomes in patients with advanced gastric cancer. Currently, surgery remains the mainstay of curative treatment. However, only an R0 resection is associated with significant cure rates, and less than half of patients with locally advanced gastric cancer will achieve an R0 resection even with aggressive surgery [2]. Despite curative resection, a large proportion of patients with locally advanced gastric cancer will experience recurrence, and the long-term survival rate remains unsatisfactory [3]. The high risk of relapse after surgery has led to the search for strategies to prevent relapse and to improve survival for gastric cancer patients, such as adjuvant therapy or neo-adjuvant approaches.

Recently, the large-scale Japanese phase III trial by the Adjuvant Chemotherapy Trial of S-1 for Gastric Cancer group reported the superiority of S-1 as an adjuvant chemotherapy over surgery alone after D2 lymph node dissection of stage II/III patients [4]. Nonetheless, even with adjuvant S-1 chemotherapy, about one-third of R0 patients died within 5 years of surgery, indicating that improved therapeutic strategies are needed.

Preoperative chemotherapy has some theoretical benefits in comparison with postoperative chemotherapy in such patients, including downstaging that increases the possibility of subsequent R0 resection, treating micrometastatic disease early in the course of therapy, evaluating susceptibility to chemotherapy, and generally better tolerability of more intensive chemotherapy. This approach is supported by a large randomized study involving 503 resectable patients; that is, the Medical Research Council Adjuvant Gastric Infusional Chemotherapy trial, the first positive neoadjuvant study, in which the effects of 3 pre- and post-operative cycles of ECF (epirubisine/cisplatin/5-FU) chemotherapy were compared with surgery alone [5]. The study concluded that perioperative chemotherapy decreased the tumor stage and improved patient survival. A similar benefit for perioperative chemotherapy was noted in a French multicenter trial in which 224 patients with potentially resectable gastric cancers were randomly assigned to receive 2–3 cycles of preoperative chemotherapy (CF, 5-FU/cisplatin) or surgery alone [6]. However, 5-year survival rates remain less than 40 % in these trials. Therefore, the development of more effective chemotherapeutic regimens would be required for further improvements of efficacy in neoadjuvant therapy.

During the last decade, several new agents with promising activity against gastric cancer have been identified. These include S-1, docetaxel, and irinotecan [7]. The therapeutic value of combination regimens including these new anticancer agents has been studied with the goal of improving overall treatment efficacy. A phase III study (V325) evaluating the impact of adding docetaxel to CF (DCF) in advanced gastric cancer showed that DCF led to significantly improved outcomes [8]. S-1 is a novel oral fluoropyrimidine, and a recent phase III trial showed that the substitution of S-1 for infusional 5-FU in the CF regimen is comparable in efficacy to 5-FU combined with cisplatin but has significant safety advantages [9]. At present, S-1 plus cisplatin (CS) is recognized as a standard treatment for unresectable advanced or recurrent gastric cancer in Japan [10].

We have previously conducted phase I and phase II studies to evaluate the effect of adding docetaxel to base treatment with S-1 plus cisplatin (DCS) to further improve the therapeutic response; both a very high response rate (87.1 %) and a promising median survival time (687 days) in patients with unresectable advanced gastric cancer were noted [11, 12]. Another phase II study of DCS with a different treatment regimen from ours has been performed by Koizumi et al. [13]; treatment was highly effective (response rate, 81 %), consistent with the results of our study. We also found an appreciable rate of downstaging (25 %) with a very high response rate and no cases of disease progression with this regimen [12], suggesting the applicability of DCS for neoadjuvant chemotherapy. Based on these encouraging results, we performed this multicenter single-arm phase II trial to evaluate the efficacy and safety of preoperative chemotherapy with DCS for locally advanced gastric cancer.

Patients and methods

Patient eligibility

Patients with locally advanced gastric cancer were eligible for the present study. Eligibility criteria included the following: age between 20 and 80 years; PS of 0-1 on the Eastern Cooperative Oncology Group (ECOG) scale;

histologically proven gastric adenocarcinoma; T3-4, N0-3, (or T2N1-3 in the case of diffuse invasive type; linitis plactica), M0 (according to the Japanese Classification of Gastric Carcinoma 13th edition) [14]; clinically diagnosed with potentially resectable tumors; no prior gastric surgery; no previous chemotherapy or radiotherapy; measurable lesion(s) or evaluable disease; no uncontrolled infectious or cardiac disease; adequate renal function; no synchronous or metachronous (within 5 years) malignancy other than carcinoma in situ; and provision of written informed consent. This study was approved by the ethics committee of each institution and hospital.

Baseline evaluation

The pre-study evaluation included physical examination, hematology, biochemistry, urinalysis, chest X-ray, and gastroduodenofiberoscopy. Gastric adenocarcinomas were staged by computed tomography (CT) scan and endoscopic ultrasound (EUS) in order to estimate primary tumor and lymph node status. *Staging* laparoscopy was performed to exclude occult M1 disease in the peritoneum or other intra-abdominal sites. Further examination using radionuclide bone scan, and/or co-registered (18F)-fluoro-2-deoxy-D-glucose (FDG) positron emission tomography (PET)/CT scan was performed if clinically indicated to exclude M1 disease.

Treatment schedule

In this multicenter, nonrandomized, open-label phase II trial, S-1 was administered orally twice daily on days 1–14 at a dose calculated according to the patient's body surface area as follows: <1.25 m^2, 40 mg; 1.25–1.5 m^2, 50 mg; and >1.5 m^2, 60 mg.

Cisplatin was administered by intravenous infusion for 2 h at 60 mg/m^2 in 5 % glucose followed by docetaxel at 60 mg/m^2 in 5 % glucose on day 8 with adequate hydration. Cycles were repeated every 3 weeks. Prophylactic administration of antiemetic medication at a standard dose was routinely used to prevent nausea and vomiting when cisplatin was administered. In the event of toxicity, the treatment delays and dose reductions were planned as previously described [12]. All patients received 2 courses of treatment, and responders received a maximum of 4 courses, followed by standard curative surgery involving a radical resection, the extent of which (total or subtotal gastrectomy) depended on the site of the primary tumor, and D2 or D3 lymphadenectomy within 4–8 weeks.

Assessment and follow-up

Toxicity was evaluated according to the Common Toxicity Criteria for Adverse Events (version 3.0). Assessment of response to neoadjuvant therapy was performed after each preoperative cycle according to Response Evaluation Criteria in Solid Tumors guidelines (version 1.0) and for primary lesions according to the guidelines of the Japanese classification of gastric carcinoma [15]. The pathological response to chemotherapy was classified according to the following criteria provided by the Japanese Gastric Cancer Association (JGCA) [16]: grade 0, no part of tumor affected; grade 1a, less than one-third affected; grade 1b, between one-third and two-thirds affected; grade 2, between two-thirds and entire tumor affected; and grade 3, no residual tumor. A pathological response was defined as one-third or more of the tumor affected (grade 1b, 2 or 3). Each patient was assessed at 1, 3, 6, 9, and 12 months, then every 6 months for 5 years, and then annually or until death.

Immunohistochemistry for ERCC1 and DDB2

Paraffin-embedded tissue sections of gastric cancer tissue were deparaffinized in xylene and treated for 20 min with 0.6 % H_2O_2 to block endogenous peroxidase activity. They were incubated overnight at 4 °C in a 1:100 dilution of mouse monoclonal antibody against ERCC1 (sc-56386, Santa Cruz Biotechnology, Santa Cruz, CA, USA) or rabbit anti-DDB2 antibody (ab77765, Abcam, Cambridge, UK). Binding of the primary antibody was detected by peroxidase staining with an avidin–biotin complex system (Dako, Carpinteria, CA, USA). Staining was graded for intensity of staining (1, weak; 2, moderate; 3, strong) and percentage of cells stained (1, 0 to <10 %; 2, 10 to <50 %; 3, 50–100 %). We classified ERCC1 and DBB2 staining as positive when tumor cells showed nuclei reactivity and both scores were two or above, as described previously [17].

Statistical methods

The primary endpoint was the R0 resection rate. The secondary endpoints were pathological response rate, response to chemotherapy, progression-free (PFS) and overall survival (OS), and chemotherapy-related toxicity. Given that the expected rate of R0 resection is 85 % and the threshold incidence is 65 %, based on previously reported data for R0 resection rates in this population [18–20], with an alpha value of 0.025 (1-sided) and a beta value of 0.2, the required number of patients was determined to be 36. The target number of patients was therefore set at 40, accounting for expected dropouts and excluded patients. PFS was defined as the time from registration until objective tumor progression or death. OS was defined as the time from registration until death from any cause. The Fisher's exact probability test was employed for